AN EFFICIENT ALGORITHM FOR COMPUTING QFT BOUNDS[1]

J. M. Rodrigues[2], Y. Chait[3,4] and C.V. Hollot[5]
University of Massachusetts
Amherst, Massachusetts, 01003

ABSTRACT

An important step in Quantitative Feedback Theory (QFT) design is the translation of closed-loop performance specifications into *QFT bounds*. These bounds, domains in a Nichols chart, serve as a guide for shaping the nominal loop response. Traditionally, QFT practitioners relied on manual manipulations of plant templates on Nichols charts to construct such bounds, a tedious process which has recently been replaced with numerical algorithms. However, since the plant template is approximated by a finite number of points, the QFT bound computation grows exponentially with the fineness of the plant template approximation. As a result, the designer is forced to choose between a coarse approximation to lessen the computational burden and a finer one to obtain more accurate QFT bounds. To help mitigate this tradeoff, this paper introduces a new algorithm to more efficiently compute QFT bounds. Examples are given to illustrate the numerical efficiency of this new algorithm.

---

[1]This work was supported in part by a National Science Foundation grant MSS-9313764 and a University of Massachusetts grant FRG/1-03477. This support is greatly appreciated.
[2]Graduate Research Assistant, Mechanical and Industrial Engineering Department; Presently a System Applications Engineer at Andover Control, Andover, MA.
[3]Associate Professor, Mechanical and Industrial Engineering Department, chait@ecs.umass.edu
[4]Author to whom all correspondence should be made to.
[5]Associate Professor, Electrical and Computer Engineering Department, hollot@ecs.umass.edu

1. INTRODUCTION

The Quantitative Feedback Theory (QFT) is an engineering design technique for uncertain feedback systems; see Horowitz (1992) for an exposition of QFT. A key step in any QFT design is the translation of closed-loop frequency-domain specifications into Nichols chart domains specifying the allowable range of the nominal open-loop response. These domains are referred to as *QFT bounds*. The design is completed when a nominal loop transmission is shaped which achieves nominal closed-loop stability and lies within its QFT bounds.

Traditionally, QFT bounds have been computed using manual graphical manipulations of plant templates on a Nichols chart. A *plant template* is a set of complex numbers representing the frequency response of an uncertain plant at a fixed frequency. Recently, algorithms have been developed for automatic computation of these QFT bounds. For example, Lomgdon and East (1978) and Thompson and Nwokah (1989) use a polygonal approximation of the plant template to simplify the computations, while Jayasuriya (1990) exploits the geometrical interpretation of the closed-loop constraint. In Wang et al. (1991), quadratic inequalities are introduced to compute QFT bounds for closed-loop specifications involving gain-phase margins, sensitivity and complementary sensitivity functions. While they have been used by various researchers in limited contexts (e.g., Jayasuriya, 1990, Nordgren, et al., 1995), Chait and Yaniv (1993), Yaniv and Chait (1993), and Chait et al. (1995), developed quadratic inequalities for general settings including continuous and discrete-time systems, as well as for parametric and non-parametric uncertainty models. These quadratic inequalities form the basis for QFT bound computations and are used in the QFT Toolbox for MATLAB Borghesani et al. (1995). However, as we explain next, these algorithms suffer a tradeoff between computational complexity and the accuracy of the QFT bound.

As explained above, forming plant templates is the starting point for computing QFT bounds. For many practical problems, however, plant templates are difficult, if not impossible, to analytically describe. Consequently, algorithms for computing QFT bounds usually rely on an approximation of the plant template by a finite number of points. For example, given the plant family

$$\mathcal{G} = \left\{ G(s) = \frac{k}{(s+a)}: \quad k \in [1,3], a \in [4,7] \right\}$$

and frequency ω, the template $\mathcal{G}_\omega = \left\{ G(j\omega): \quad G(s) \in \mathcal{G} \right\}$ can be approximated by the 12-point set

$$\tilde{\mathcal{G}}_\omega = \left\{ G(j\omega) = \frac{k}{j\omega + a}: \quad k \in \{1,2,3\}, a \in \{4,5,6,7\} \right\}$$

Forming QFT bounds requires evaluations (of a quadratic constraint as we show later) at each point of the plant template approximation. Thus, the number of evaluations grows with the fineness of the approximation, and, as one might expect, coarse plant template approximations can lead to erroneous conclusions about robust performance. For instance, consider a single-loop system with plant family $\mathcal{G}$, controller K(s), performance weight W(ω) and a robust performance specification involving the sensitivity

$$\left|\frac{1}{1+K(j\omega)G(j\omega)}\right| \leq W(\omega), \quad \forall\omega, \forall G \in \mathcal{G} \tag{1}$$

With K(s)=1 and for some ω, suppose the plant template $\mathcal{G}_\omega$ is the arc (solid line) in Fig. 1. The specification (1) is satisfied if $\mathcal{G}_\omega$ does not enter the disk centered at (-1,0) with radius $W^{-1}(\omega)$. Clearly, (1) is not met. However, when we use a coarse approximation of $\mathcal{G}_\omega$, say the 3-point $\tilde{\mathcal{G}}_\omega$ denoted by 'o's shown in Fig. 1, it appears that (1) is satisfied. As expected, using a finer approximation such as the 10-point $\tilde{\mathcal{G}}_\omega$ denoted by 'x's indicates that (1) is indeed violated. Though the use of a 3-point $\tilde{\mathcal{G}}_\omega$ here is extreme, it does illustrate the need for an accurate approximation of plant templates.

Another factor to be considered in approximating plant templates is that in most practical cases, only the *boundary* of the plant template is needed for computing QFT bounds. That is, if the plant template $\mathcal{G}_\omega$ is a closed, connected set, then performance specifications like (1) enjoy the following property:

$$\left|\frac{1}{1+K(j\omega)G(j\omega)}\right| \leq W(\omega), \quad \forall G(j\omega) \in \mathcal{G}_\omega$$

if and only if

$$\left|\frac{1}{1+K(j\omega)G(j\omega)}\right| \leq W(\omega), \quad \forall G(j\omega) \in \partial\mathcal{G}_\omega$$

where $\partial\mathcal{G}_\omega$ is the boundary of the plant template $\mathcal{G}_\omega$. This follows from an application of the Maximum Modulus Theorem (Chait et al., 1995). As a consequence, it is important that the approximation $\tilde{\mathcal{G}}_\omega$ is formed from only from $\partial\mathcal{G}_\omega$. The interior of $\mathcal{G}_\omega$ does not contribute towards the QFT bound and only increases the computational load.

In summary, we have discussed issues in using plant template approximations in computing QFT bounds. The tradeoff between coarse approximations and QFT bound accuracy is our main motivation. The purpose of this paper is to present an efficient algorithm for evaluating QFT bounds from a given $\tilde{\mathcal{G}}_\omega$. This increased efficiency will allow the designer to consider finer approximations of plant templates and hence more accurate QFT bounds. The next section formally introduces the notion of QFT bounds.

2. QFT BOUNDS

Let some performance function F(s) involving the controller K(s) be given as well as a performance weight W(s), plant set $\mathcal{G}$ of transfer functions and nominal plant $G_0(s)$. For a fixed frequency ω, the *QFT bound* (for the nominal loop $G_0(s)K(s)$) is the set of complex numbers $G_0(j\omega)\mathcal{K}_\omega$ satisfying:

$$\begin{gathered} \left|F(j\omega)\right| \le W(\omega), \quad \forall G(j\omega) \in \mathcal{G}_\omega \\ \Leftrightarrow \\ G_0(j\omega)K(j\omega) \in G_0(j\omega)\mathcal{K}_\omega \end{gathered}$$

Said another way, $\mathcal{K}_\omega$ is the set of controller gains and phases which lead to satisfaction of the algebraic constraint $|F(j\omega)| \le |W(j\omega)|$.

Quadratic Inequalities. Algorithms used to compute QFT bounds are based on so-called quadratic inequalities; see Chait and Yaniv (1993), Yaniv and Chait (1993), and Chait et al. (1995). To see how quadratic inequalities arise in the computation of QFT bounds, assume that F(s) is the closed-loop sensitivity function $S(s) = (1+G(s)K(s))^{-1}$ and $\mathcal{G}_\omega$ is approximated by the n-point set $\tilde{\mathcal{G}}_\omega = \{G_1(j\omega), G_2(j\omega), \ldots, G_n(j\omega)\} \subset \mathcal{G}_\omega$. The sensitivity reduction specification with respect to $\tilde{\mathcal{G}}_\omega$ is

$$\left|\frac{1}{1+K(j\omega)G(j\omega)}\right| \le W(\omega), \quad \forall\, G \in \tilde{\mathcal{G}}_\omega \tag{2}$$

Substituting the polar forms

$$K(j\omega) = k(\omega)e^{j\theta(\omega)}, \quad G_i(j\omega) = g_i(\omega)e^{j\varphi_i(\omega)}, \quad i = 1, \ldots, n$$

into (2) and simplifying results in a set of *quadratic inequalities*

$$g_i^2(\omega)k^2(\omega) + 2g_i(\omega)\cos(\varphi_i(\omega) + \theta(\omega))k(\omega) + 1 - \frac{1}{W^2(\omega)} \ge 0, \quad i = 1, \ldots, n \tag{3}$$

It can be shown that typical performance specifications, such as those placed on complementary sensitivity or on control effort, can be transformed into such quadratic inequalities; e.g., see Chait and Yaniv (1993). Suppressing the dependence on ω, the general form for these quadratic inequalities are denoted by

$$p_i(k,\theta) \equiv a_i(\theta)k^2 + b_i(\theta)k + c_i(\theta) \geq 0, \quad i = 1,\ldots,n \tag{4}$$

with the associated QFT bound $G_0(j\omega)\mathcal{K}_\omega$ where

$$\mathcal{K}_\omega = \bigcap_{i=1,\ldots,n} \mathcal{K}_\omega^i$$

and

$$\mathcal{K}_\omega^i = \left\{ ke^{j\theta}: \quad p_i(k,\theta) \geq 0 \right\} \tag{5}$$

We say that $G_0(j\omega)\mathcal{K}_\omega^i$ is the *QFT bound associated with the i'th quadratic constraint* in (3). Typically, $\mathcal{K}_\omega$ is computed over a grid of the controller phase θ ranging in [0,2π). For fixed $\theta \in [0,2\pi)$, we define

$$\mathcal{K}_{\omega,\theta} = \left\{ k \geq 0: \quad p_i(k,\theta) \geq 0,\ i = 1,\ldots,n \right\}$$

and

$$\mathcal{K}^{i}_{\omega,\theta} = \left\{ k \geq 0: \quad p_i(k,\theta) \geq 0 \right\}$$

which in turn satisfy

$$\mathcal{K}_{\omega,\theta} = \bigcap_{i=1,\ldots,n} \mathcal{K}^{i}_{\omega,\theta}, \qquad \mathcal{K}^{i}_{\omega} = \bigcup_{\theta\in[0,2\pi)} \mathcal{K}^{i}_{\omega,\theta}$$

and

$$\mathcal{K}_{\omega} = \bigcup_{\theta\in[0,2\pi)} \bigcap_{i=1,\ldots,n} \mathcal{K}^{i}_{\omega,\theta}$$

For fixed ω and θ, the i'th QFT bound $G_0(j\omega)\mathcal{K}^{i}_{\omega,\theta}$ is computed by considering the real roots of the quadratic equality $p_i(k,\theta)=0$. These roots define the boundary of $\mathcal{K}^{i}_{\omega,\theta}$ and together with the direction of the parabola $p_i(k,\theta)=0$ completely describe $G_0(j\omega)\mathcal{K}^{i}_{\omega,\theta}$. Algorithms for computing QFT bounds typically include the following steps:

<u>Algorithm 1</u>

1. Establish a frequency grid $\Omega \in R^{+}$ and a controller phase grid $\Theta \in [0,2\pi)$.

   2. Fix $\omega \in \Omega$.

      3. Fix $\theta \in \Theta$.

         4a. Evaluate the coefficients of $p_i(k,\theta)$ in (4) for all points in $\tilde{\mathcal{P}}_{\omega}$.

4b. Evaluate the roots of $p_i(k,\theta)=0$, i=1,…,n.

4c. Compute the QFT bounds $\mathcal{K}^i_{\omega,\theta}$.

4d. Compute $\mathcal{K}_{\omega,\theta}$ from $\cap \mathcal{K}^i_{\omega,\theta}$.

5. Repeat 3 until Θ is emptied.

6. Evaluate $\mathcal{K}_\omega$ from $\cup \mathcal{K}_{\omega,\theta}$.

7. Repeat 2-6 until Ω is emptied.

The main result of this paper gives a new algorithm for computing $\mathcal{K}_\omega$. It exploits the real root version of the Edge Theorem (Bartlett et al., 1988) in Step 4b to reduce the number of points in $\tilde{\mathcal{P}}_\omega$ that need to be evaluated. Before getting to this algorithm we briefly present some notions on convex sets which are necessary in explaining the Edge Theorem and the modification to Algorithm 1.

3. CONVEX SETS AND EDGE THEOREM

Let *S* be a subset of the plane, then *S* is said to be *convex* if the line joining any two points in *S* remains in *S*. The *convex hull* of *S*, denoted by *conv S*, is the smallest convex set containing *S*. If *S* consists of a finite number of points, then *conv S* is called a *polytope*. A polytope has several sets of distinguished points: vertices and edges. Since we consider only polytopes in the plane these points are easily illustrated in Fig. 2. The collection of polytope edges and vertices is denoted by $\mathcal{E}$(P) and *ver* P, respectively.

Now, consider a set of second-order polynomials

$$\left\{\rho_i(z) \equiv \alpha_i z^2 + \beta_i z + \gamma_i: \quad i = 1, \ldots, n\right\}$$

or its equivalent representation in polynomial coefficients space

$$S = \left\{(\alpha_i, \beta_i, \gamma_i): \quad i = 1, \ldots, n\right\}$$

Let P denote the *polytope of polynomials* defined by

$$P = \left\{\alpha z^2 + \beta z + \gamma: \quad (\alpha, \beta, \gamma) \in conv\, S\right\}$$

Notice that $\left\{\rho_i(z), \quad i = 1, \ldots, n\right\} \subset P$ and that every vertex of P is some $\rho_i(z)$. Let

$$\mathcal{E}(P) = \left\{\alpha z^2 + \beta z + \gamma: \quad (\alpha, \beta, \gamma) \in \mathcal{E}(conv\, S)\right\}$$

denote the *edge polynomials* of P. The *root set* of a given set of polynomials X is defined as

$$\sigma[X] = \left\{z \in C: \quad \rho(z) = 0, \rho(z) \in X\right\}$$

Let $\partial\sigma[X]$ denote the *boundary* of $\sigma[X]$ and $\sigma_R[X]$ that subset of $\sigma[X]$ which is real; i.e.,

$$\sigma_R[X] = \{z \in \sigma[X]: \quad Im\, z = 0\}$$

We say that $\sigma_R[X]$ is the real root set of *X*. The real root version of the Edge Theorem states that the real root set of a polytope of polynomials is equal to the real root set of the edges (Bartlett et al. 1988); i.e.,

$$\sigma_R\left[P\right] = \sigma_R\left[\mathcal{E}(P)\right] \tag{6}$$

We are now in a position to describe a new algorithm for computing QFT bounds.

4. THE NEW ALGORITHM

As discussed in Section 2, the QFT bound $G_0(j\omega)\mathcal{K}^i_{\omega,\theta}$ is computed from the real roots of the quadratic equalities $p_i(k,\theta) = 0$; see (4). We now apply (6) to help find these roots without considering all i'th quadratic equalities.

Theorem 1 (Rodrigues, 1995). For fixed controller angle θ, consider the finite set of polynomials $\{p_i(k,\theta), \quad i = 1,\ldots,n\}$ introduced in (4). Let *P* denote the corresponding convex hull of polynomials. Then,

$$\partial\sigma_R[P] \subset \sigma_R[ver\, P]$$

Proof. From (6),

$$\sigma_R[P] = \sigma_R\left[\mathcal{E}(P)\right]$$

Hence,

$$\partial\sigma_R[P] = \partial\sigma_R\left[\mathcal{E}(P)\right]$$

To complete the proof we show that

$$\partial\sigma_R\left[\mathcal{E}(P)\right] = \sigma_R\left[\,ver\ P\right] \tag{7}$$

To this end, consider a typical edge of *P*:

$$\left\{(1-\lambda)p_i(k,\theta) + \lambda p_j(k,\theta):\ \lambda \in [0,1],\ p_i(k,\theta), p_j(k,\theta) \in ver\ P\right\} \tag{8}$$

The roots of $(1-\lambda)p_i(k,\theta) + \lambda p_j(k,\theta) = 0$ are precisely the solutions of the root locus

$$1 + \frac{\lambda}{\lambda - 1}\frac{p_j(k,\theta)}{p_i(k,\theta)} = 0$$

as the root locus variable $\frac{\lambda}{\lambda - 1}$ ranges over $[0,\infty)$. From root locus arguments, the real portion of the loci is bounded by the real roots of $p_i(k,\theta)$ and $p_j(k,\theta)$. Thus, the boundary of the real roots of (8) is contained in $\sigma_R\left[\, ver\, P\right]$. This shows (7) and completes the proof. ■

This result indicates that non-vertex polynomials (e.g., edge and interior polynomials of *P*) do not contribute towards the computation of QFT bounds and only increase the computational burden. Hence, by working with convex-hull vertices, we can potentially achieve a reduction in the computational burden. As a result, the designer can consider finer approximations of plant templates without expecting a commensurate increase in computation since many of the resulting quadratic inequalities would be removed prior to the QFT bound computation. An additional reduction in the number of quadratic inequalities can be expected due to the fact that the plant template boundary may not be entirely mapped into polytope vertices; see Barmish (1994, pg. 142) for an explanation for this fact and Example 2 below for an illustration. A modified algorithm for computing QFT bounds utilizing Theorem 1 is described by:

<u>Algorithm 2</u>

1. Establish a frequency grid $\Omega \in R^+$ and a controller phase grid $\Theta \in [0,2\pi)$.
2. Fix $\omega \in \Omega$.
3. Fix $\theta \in \Theta$.
   4a. Evaluate the coefficients of $p_i(k,\theta)$ in (4) for all points in $\tilde{\mathcal{G}}_\omega$.
   4b. Evaluate the *polytope of polynomials* $P = conv\left\{p_i(k,\theta):\ \ i=1,\ldots,n\right\}$
   4c. Evaluate the roots of $p_i(k,\theta) = 0$, $p_i(k,\theta) \in P$.

4d. Compute the QFT bounds $\mathbb{X}^{i}_{\omega,\theta}$ for each vertex of *P*.

4e. Compute $\mathbb{X}_{\omega,\theta}$ from $\cap \mathbb{X}^{i}_{\omega,\theta}$.

5. Repeat 3 until Θ is emptied.

6. Evaluate $\mathbb{X}_{\omega}$ from $\cup \mathbb{X}_{\omega,\theta}$.

7. Repeat 2-6 until Ω is emptied.

The twist in this algorithm is the use of Theorem 1 to reduce the number of operations in steps 4c-4e. Of course, identifying the vertices required in step 4b is an additional computational load, however, as we show in the next section, this increase appears to be offset by a reduction in the number of quadratic equalities which are ultimately evaluated.

5. EXAMPLES

In this section we give two examples to compare the efficiency of existing algorithms (e.g., Algorithm 1) for computing QFT bounds with the new algorithm (Algorithm 2). Both algorithms were implemented and solved using the QFT Toolbox for MATLAB (Borghesani et al. (1995). The convex-hull vertices were identified using software from Schreier (1995). For a meaningful comparison, the two algorithms were compared by counting the number of floating point operations, *flops*, a measure consistent from one trial to another that does not depend on the computing platform.

Example 1. The first example considers systems occurring in active noise and vibration control where the plant consists of highly underdamped resonances ω_n. This example considers a plant set with only one such resonance:

$$\mathcal{G} = \left\{ G(s) = \frac{\omega_n^2}{s^2 + 2\varsigma\omega_n s + \omega_n^2} : \quad \omega_n \in [0.75, 1.25], \varsigma \in [0.02, 0.06] \right\}$$

Because plant magnitude and phase vary significantly around such a resonance, the plant template $\mathcal{G}_\omega$ is finely approximated to accurately capture variations in ζ and ω_n. Our plant template approximation is formed using a simple grid in the parameter space (ζ,ω_n) as is often done in practice. Such grids often result in template approximations $\tilde{\mathcal{G}}_\omega$ that are formed from undesirable interior points of $\mathcal{G}_\omega$. However, it is possible (in this example) to carefully grid the parameter space to exclude such interior. In more practical examples, it may be difficult to do this. For comparison purposes we use 75-element and 1000-element templates at a single frequency $\omega = 1$; see Figs. 3-4.

We consider the sensitivity reduction specification

$$|S(j\omega)| = \left| \frac{1}{1 + G(j\omega)K(j\omega)} \right| < 1.2, \quad \text{for each } G \in \mathcal{G}_\omega \tag{9}$$

The nominal plant $G_0(j\omega)$ corresponds to ζ=0.02 and ω_n=0.75. A comparison of the number of flops used at nominal loop $G_0(j\omega)K(j\omega)$ phase of -125° (i.e., θ=51°) by both algorithms for the

1000-element plant template is given in Table 1. In Algorithm 2, P had only 110 vertices compared with the 1000 quadratic inequalities evaluated in Algorithm 1. This led to a 35% reduction in flops.

Algorithm	No. of Flops
QFT Toolbox (Algorithm 1)	85,921
New algorithm (Algorithm 2)	56,266

Table 1. Comparison of algorithms at a nominal-loop phase of -125°

for the 1000-element template in Example 1

The number of vertices of P is a function of the controller phase θ. When we consider a nominal loop phase range of [0°,-360°) with a -5° grid, the number of flops decreases by 41%; see Table 2.

Algorithm	No. of Flops
QFT Toolbox (Algorithm 1)	4,952,790
New algorithm (Algorithm 2)	2,899,439

Table 2. Comparison of algorithms at a nominal-loop phase range of [0°,-360°)

for the 1000-element template in Example 1

As discussed earlier, the designer is faced with a tradeoff between a coarse plant template approximation to lessen the computational burden and a finer one to obtain more accurate QFT bounds. This tradeoff is illustrated by considering both QFT bounds evaluated with the 75-element and the 1000-element plant templates. In Fig. 5, the nominal-loop response $G_0(j1)K(j1)$ must lie above the solid line or below the dashed line. The difference due to plant template approximations is most noticeable in the lower region of the QFT bounds where peaking in $S(j\omega)$ is most sensitive to variations in $G_0(j\omega)K(j\omega)$. It is clearly seen that when the 75-element template is used, one can design a controller that violates the QFT bound computed with the 1000-element template. In this example, a worst-case sensitivity peaking of 1.36 occurs when a controller places the nominal-loop at the dot in Fig. 5.

Example 2. The plant family in our second example is

$$\mathcal{G} = \left\{ G(s) = \frac{k}{(s+a)} : \quad a \in [1,\, 5], k \in [1, 10] \right\}$$

and the specification is again given by (9). In this case, a plant template approximation formed from only boundary points of $\mathcal{G}_\omega$ was easily constructed using a 400-element grid in parameter space as shown in Fig. 6.

To illustrate the mapping of this plant template approximation to a polytope of polynomials, consider the quadratic inequalities (4) at a nominal loop phase of -180°. Because $a_i>0$ for all i=1,…,n, we can normalize the polynomial coefficients as follows

$$a_i k^2 + b_i k + c_i \geq 0 \iff k^2 + \underline{b}_i k + \underline{c}_i \geq 0$$

where $\underline{b}_i = b_i/a_i$ and $\underline{c}_i = c_i/a_i$. The plant template approximation in Fig. 6 generates the set of coefficients $(\underline{b}_i, \underline{c}_i)$ denoted by 'x's in Fig. 7. The boundary of the associated convex hull is denoted by the solid-line segments. Only the vertices of the polytope contribute to the QFT bound computation; the rest of the boundary and the polytope interior can be safely ignored in the computations.

Table 3 shows that the new algorithm is more efficient even though: (1) the plant template approximation (see Fig. 6) uses no interior of $\mathcal{G}_{\omega}$, and (2) it requires additional overhead associated with computation of the convex hull.

Algorithm	No. of Flops
QFT Toolbox (Algorithm 1)	1,473,879
New algorithm (Algorithm 2)	1,359,710

Table 3. Comparison of algorithms at a nominal-loop phase range [0°,-360°)

for the 400-element template in Example 2

6. CONCLUSIONS

The QFT technique is gaining increased recognition as an effective tool for control design. However, QFT design involves approximations which can influence whether the controller meets the original design specifications. This paper presents a new algorithm for computing QFT bounds which provides the designer with improved trade-off in choosing between a coarse plant template approximation to minimize the computational burden and a fine approximation to increase the accuracy of the QFT bounds. This algorithms has an immediate impact to a number of QFT design papers that involve bound computation via quadratic inequalities.

7. REFERENCES

Barmish, B.R., 1994, *New Tools for Robustness of Linear Systems*, Macmillan Pub. Co., New York.

Bartlett, A.C., Hollot, C.V., and Huang, L., 1988, "Root Locations of an Entire Polytope of Polynomials: It Suffices to Check the Edges*," Mathematics of Control, Signals and Systems*, Vol. 1, pp. 61-71.

Borghesani, C., Chait, Y., and Yaniv. O*.,* 1995, *The Quantitative Feedback Theory Toolbox for MATLAB*, The MathWorks, MA.

Chait, Y., and Yaniv, O., 1993, "Multi-Input/Single-Output Computer-Aided Control Design Using the Quantitative Feedback Theory," *Int. J. Robust and Nonlinear Control*, Vol. 3, pp. 47-54.

Chait, Y., Borghesani, C., and Zheng, Y., 1995, "Single-loop QFT design for robust performance in the presence of non-parametric uncertainties," *J. Dynamic Systems, Measurements, and Control*, Vol. 117, pp. 420-424.

Horowitz, I.M., 1992, *Quantitative Feedback Theory (QFT)*, QFT Publications, 4470 Grinnell Ave., Boulder, Colorado, 80303.

Jayasuriya, S., 1990, "QFT Type Design for Maximizing Tolerable Disturbances in Structured Uncertain Systems," in *Recent Developments in Quantitative Feedback Theory*, Ed. O.D.I. Nwokah, ASME Pubs., pp. 51-58.

Longdon, L., and East, D.J., 1978, "A Simple Geometrical Technique for Determining Loop Frequency Response Bounds Which Achieve Prescribed Sensitivity Specifications," *Int. J. Control,* Vol. 30(1), pp. 153-158.

Nordgren, R.E., Franchek, M.A., and Nwokah, O.D.I., 1995 ,"A Design Procedure for the Exact H-infinity Robust Performance Problem,", *Int. J. Robust & Nonlinear Control*, Vol. 5, pp. 107-118.

Rodrigues, J.M., 1995*, Toward Exorcising the Curse of Dimensionality from Bound Computation in the Quantitative Feedback Theory*, M.S. Thesis, Department of Mechanical and Industrial Engineering, University of Massachusetts, Amherst.

Schreier, R., 1995, *Computing the Convex Hull in 2 Dimensions*, a shareware MATLAB code, Oregon State University.

Thompson, D.F., and Nwokah. O.D.I., 1989, “Stability and Optimal Design in Qualitative Feedback Theory,” presented at the ASME Winter Annual Meeting*, ASME paper 89-WA/DSC-39*.

Wang, G.G., Chen, C.W., and Wang S.H., 1991, “Equations for Loop Bound in Quantitative Feedback Theory,” *Procs. Conf. On Decision and Control*, pp. 2968-2969.

Yaniv, O., and Chait, Y., 1993, “Direct Control Design in Sampled-Data Uncertain Systems,” *Automatica*, Vol. 29, pp. 365-372.

LIST OF FIGURES

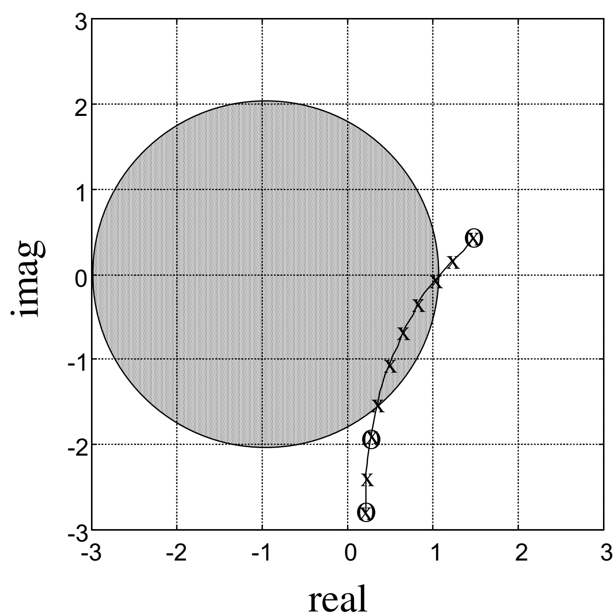

Figure 1: Graphical interpretation of (1)

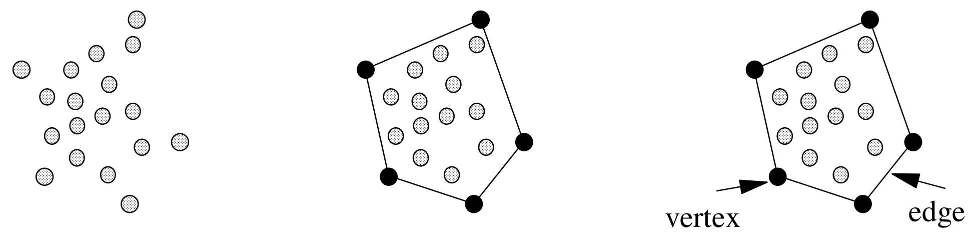

Figure 2: A finite set of points S (left), *conv* S (middle) and vertices and edges of *conv* S (right)

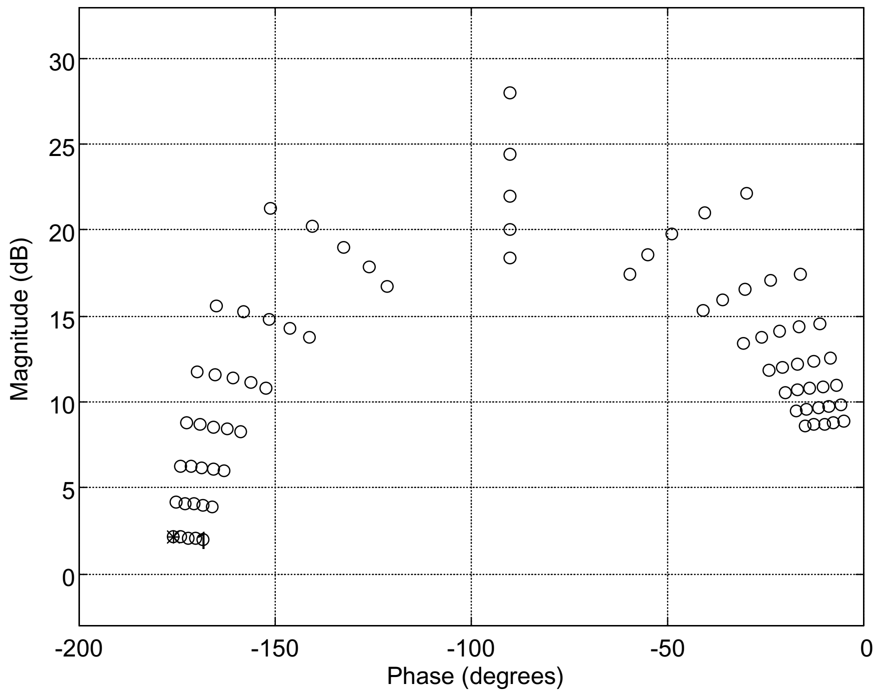

Figure 3: The 75-element plant template in Example 1

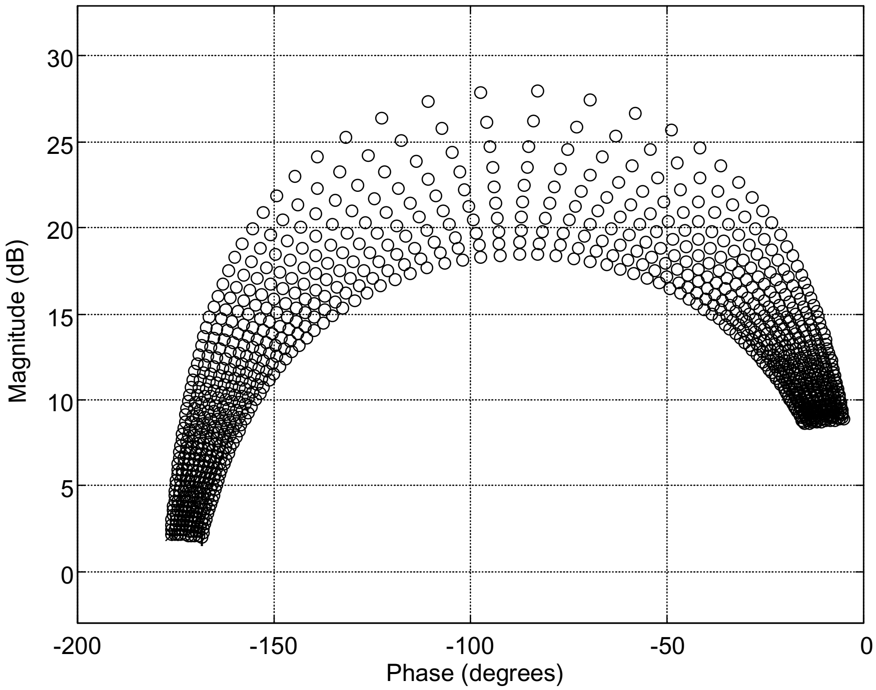

Figure 4: The 1000-element plant template in Example 1

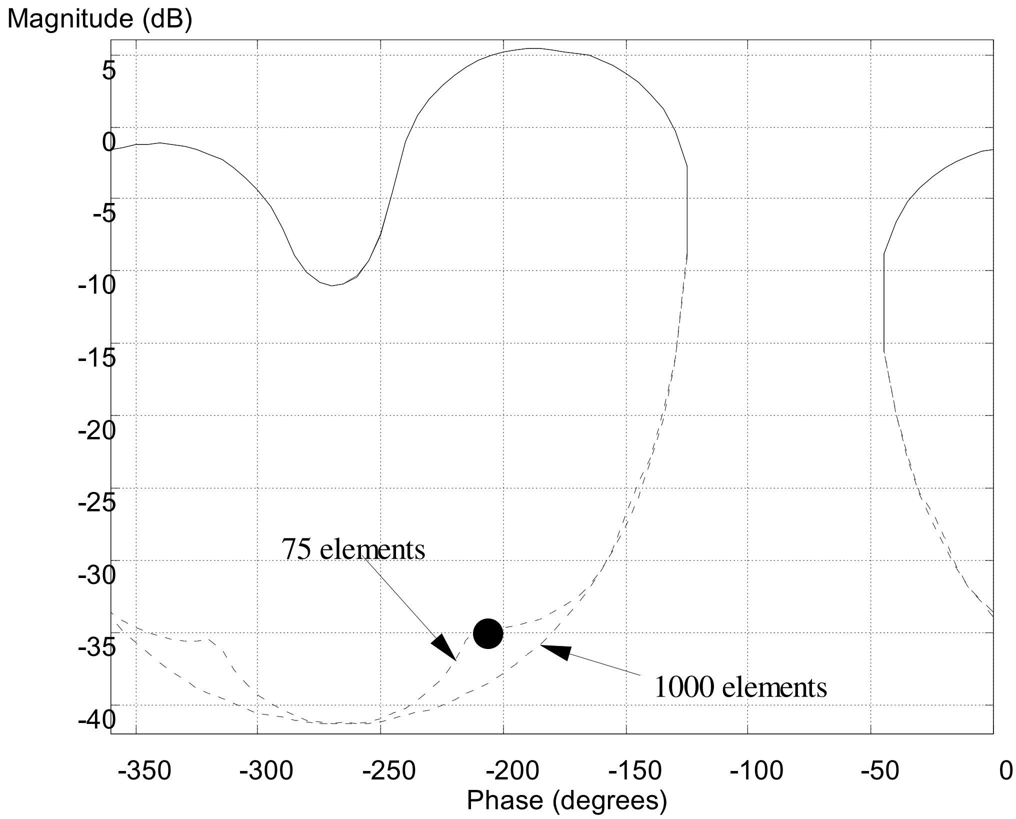

Figure 5: Comparing QFT bounds computed for the 1000-element and 75-element templates

in Example 1

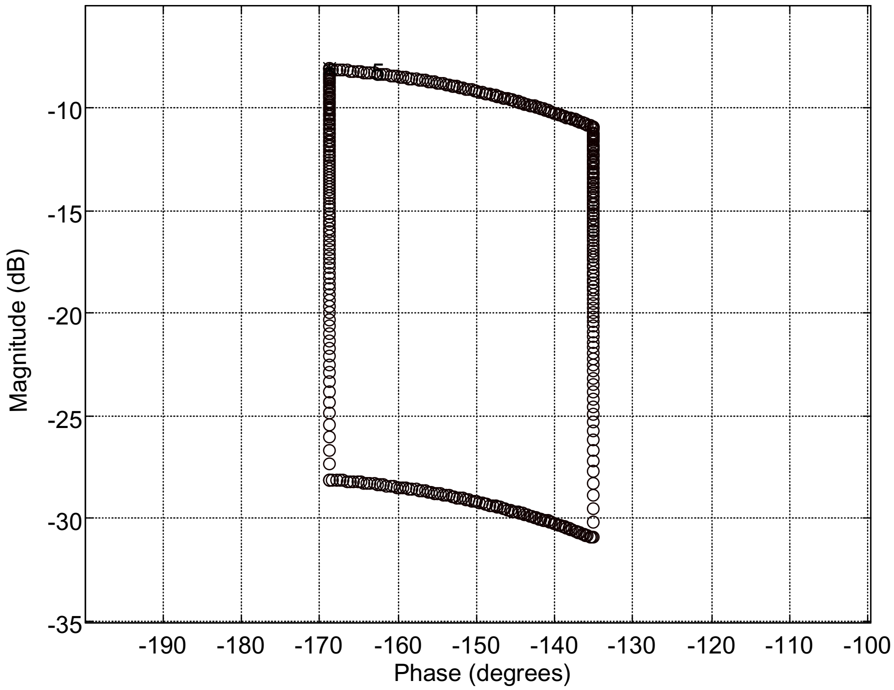

Figure 6: The 400-element plant template at $\omega = 5$ in Example 2

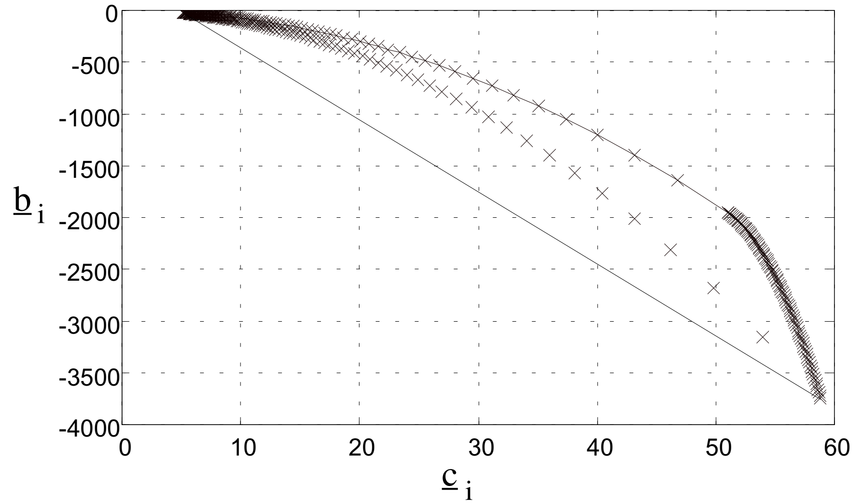

Figure 7: The polynomial coefficients space at a nominal-loop phase of -180° in Example 2